Understanding S-shaped current-voltage characteristics of organic solar cells: Direct measurement of potential distributions by scanning Kelvin probe

Cite as: Appl. Phys. Lett. **103**, 243303 (2013); https://doi.org/10.1063/1.4846615
Submitted: 25 October 2013 . Accepted: 27 November 2013 . Published Online: 11 December 2013

Rebecca Saive, Christian Mueller, Janusz Schinke, Robert Lovrincic, and Wolfgang Kowalsky

Understanding S-shaped current-voltage characteristics of organic solar cells: Direct measurement of potential distributions by scanning Kelvin probe

Rebecca Saive,[1,2,3,a)] Christian Mueller,[1,3] Janusz Schinke,[1,2] Robert Lovrincic,[1,2] and Wolfgang Kowalsky[1,2,3]
[1]*InnovationLab GmbH, 69115 Heidelberg, Germany*
[2]*Institut für Hochfrequenztechnik, TU Braunschweig, 38106 Braunschweig, Germany*
[3]*Kirchhoff-Institute for Physics, Heidelberg University, 69120 Heidelberg, Germany*

(Received 25 October 2013; accepted 27 November 2013; published online 11 December 2013)

We present a comparison of the potential distribution along the cross section of bilayer poly (3-hexylthiophene)/1-(3-methoxycarbonyl)propyl-1-phenyl[6,6]C61 (P3HT/PCBM) solar cells, which show normal and anomalous, S-shaped current-voltage (IV) characteristics. We expose the cross sections of the devices with a focussed ion beam and measure them with scanning Kelvin probe microscopy. We find that in the case of S-shaped IV-characteristics, there is a huge potential drop at the PCBM/Al top contact, which does not occur in solar cells with normal IV-characteristics. This behavior confirms the assumption that S-shaped curves are caused by hindered charge transport at interfaces. © *2013 AIP Publishing LLC*. [http://dx.doi.org/10.1063/1.4846615]

As the demand for renewable energy sources increases continuously, organic solar cells become more and more interesting as cheap and lightweight energy suppliers. The efficiency and lifetime increases incessantly and commercial applications can already be found. In contrast to inorganic semiconductors, the physics of organic electronic devices still lack a closed description. The phenomenological specifications of the properties are step by step supported by fundamental research.

A major obstacle for both research and potential applications is the poor reproducibility of spin coated polymer solar cells. A common phenomenon for these cells is so called S-shaped current-voltage (IV) characteristics. The IV-curve under illumination shows a kink between the first and the fourth quadrant,[1] which leads to a reduced fill factor and usually to a reduced open circuit voltage.[2] Many experiments[3,4] as well as simulations[5] attributed this behavior to restricted charge transport at the interfaces. Others suggested a vertical phase separation of the fullerenes away from the cathode as cause for S-shaped IV-curves.[6] This unfavorable phase segregation would hinder electron extraction at the cathode from the PCBM component.[6] For planar junctions, an imbalance of the individual charge carrier mobilities has been presented as the culprit,[7] but that does not appear to extend to typical bulk heterojunctions (BHJs).[5]

We apply scanning Kelvin probe microscopy (SKPM) to cross sections of bilayer poly(3-hexylthiophene)/1-(3-methoxycarbonyl)propyl-1-phenyl[6,6]C61 (P3HT/PCBM) solar cells with normal and S-shaped IV-characteristics to measure the potential distribution in these devices along the charge transport path and therefore gain a direct insight into the dominating transport barriers. Using bilayer rather than BHJ cells as model system enables us to clearly rule out contributions from a random morphological distribution of the active materials. We are able to directly observe an increased transport barrier at the PCBM/cathode interface for solar cells with S-shaped IV-characteristics, indicating a non ideal cathode interface as the origin for the S-shaped IV-characteristics.

The solar cells were prepared on indium-tin oxide (ITO) coated and patterned glass substrates by spin coating of the active materials. First, a poly(3,4-ethylenedioxythiophene):poly-(styrenesulfonate) (PEDOT:PSS) buffer layer was spin coated on top of the ITO electrode. P3HT was solved in chlorobenzene and spin coated with 1000 RPM for 90 s on top of the PEDOT:PSS. As proposed by Ayzner *et al.*,[8] the PCBM was solved in dichloromethane to gain well separated layers. It was spin coated with 4000 RPM for 10 s. From analytical transmission electron microscopy (TEM) measurements[9] on our samples, we certainly know that the P3HT and PCBM form well separated layers. The whole preparation was performed in a glove box under nitrogen atmosphere. 0.6 nm LiF and 100 nm Al were thermally evaporated to form the top contact. Some of our solar cells showed S-shaped IV-curves caused by a temporary iodine contamination of our glove box, which we found out by XPS measurements. We prepared four batches of bilayer solar cells. The first and the third one were prepared in a clean glove box and the second and fourth in a contaminated glove box. In the first and the third batch, all solar cells showed normal IV-characteristics; in the second and fourth batch, all solar cells showed S-shaped IV-curves.

For further treatment and characterization, we use a measurement setup, which consists of a combined crossbeam scanning electron microscope (SEM) and a focused ion beam (FIB) with an implemented scanning probe microscope (SPM) (Zeiss/DME BRR, see Ref. 10 for details). We lay the cross section of the samples open by milling micrometer sized holes with the FIB. The obtained cross sections are very smooth[11] and feasible to address by SPM methods like SKPM. We run the SKPM measurements in a one pass

[a)]Author to whom correspondence should be addressed. Electronic mail: rebecca.saive@innovationlab.de

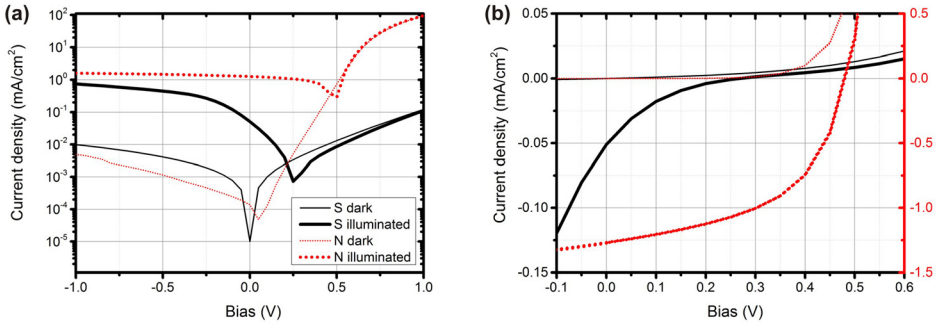

FIG. 1. (a) IV-curves in the dark and under non standard illumination on a logarithmic scale of sample S (black solid line) and sample N (red dashed line). (b) Zoom into the active region of the solar cells. Sample S refers to the left (black) y-axis, sample N to the right (red) y-axis. Sample S exhibits an S-shaped characteristic under illumination.

amplitude modulated manner. As the SPM is implemented into the SEM/FIB system, preparation and analysis of the cross sections can be performed *in-situ*. The Ga FIB is known to change material properties due to Ga implantation and destruction of molecules and can also dope organic semiconductors.[12] Therefore, we compared the IV curves of our solar cells before and after FIB milling[10] and observed no altering. Furthermore, we prepared the cross sections by cleaving and microtome cutting and compared the results.[11] We gained similar potential distributions for all preparation methods.[11] The samples were electrically contacted in the microscope and a light emitting diode was mounted below the samples such that IV-curves in the dark and under (non standard) illumination could be recorded.

Figure 1(a) shows the IV-curves captured in the dark and under illumination of sample S (black solid line) and sample N (red dashed line) in a logarithmic scale. The forward current for sample S is three orders of magnitude lower than that of sample N, already hinting to a hindered charge transport in the case of S. Figure 1(b) zooms into the active region of the solar cells to demonstrate the S-shaped character of the IV-curves of sample S. Sample S refers to the left (black) y-axis, sample N to the right (red) y-axis.

SKPM measurements of the samples have been performed under bias voltages between −1 V and 1 V in the dark and under illumination. For each bias voltage, a two dimensional scan field of the topography and the surface potential was captured. From these scans, profiles of the surface potential were extracted (see Ref. 10 for details). Figure 2 shows an SKPM measurement of sample S without applied bias voltage (both electrodes grounded) from which the 0 V profile was extracted. The substrate, the ITO, the organic layer, and the Al can be clearly identified. A differentiation of the P3HT and the PCBM is not possible as their work functions measured by Kelvin probe are very similar.[13] As expected, the measured work function of Al is smaller than that of ITO. The difference amounts to ca. 0.5 V, which reasonably corresponds to the open circuit voltage of the solar cells.

In Figure 3, the surface potential distributions of (a) sample S and (b) sample N are shown for bias voltages of −1 V, −0.5 V, 0 V, 0.5 V, and 1 V. The data result from measurements in the dark, illumination had no visible influence on the profiles under bias voltage. In the diagrams, the regions of the ITO, the bilayer, and the aluminum are marked. The measured surface potential is a superposition of the work function difference between the SKPM cantilever and the sample and the applied bias voltage. That means that the 0 V profiles depict the work function of the samples plus or minus a constant value, which is determined by the cantilever. The work function measurements were similar for all measured devices, regardless if a normal or S-shaped IV-characteristic was measured for the device. With an applied bias voltage, the situation changes: In sample S, the potential lines run parallel from the ITO through the bilayer to the aluminum and drop there to the ground potential value. In sample N, the potential lines already run together at the ITO/P3HT contact and in the bilayer.

To gain a better view on the net voltage drop in the cell, the work function (signal at 0 V bias voltage) can be subtracted. In Figure 4, the net (relative) potential profile for sample S (black solid line) and sample N (red dashed line) is shown at bias voltages of −1 V and 1 V, respectively. The layer thicknesses were not identical in both samples. Furthermore, the absolute change of the measured potential is always smaller than the applied voltage, which is a known SKPM measurement artifact[14] and not identical in both measurements. To simplify the comparison, two different coordinate systems were used. The lower x-axis and the left y-axis (both in black) refer to sample S, and the upper x-axis and the right y-axis (both in red) refer to sample N. Again the regions of the ITO, the bilayer, and the aluminum are drafted. In this presentation, it becomes clear that the potential distributions in the two devices are entirely different. In sample N, the potential drops both at the interface between

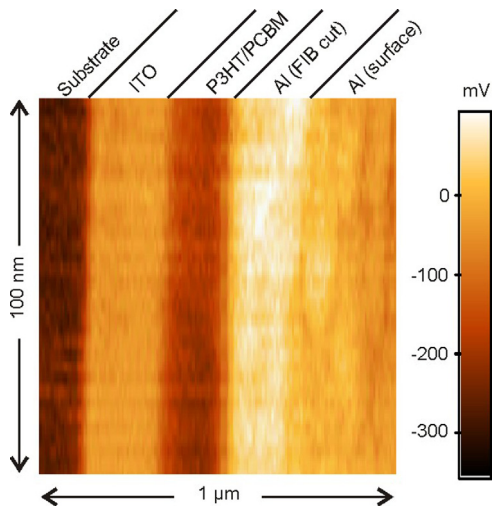

FIG. 2. SKPM measurement of the cross section of sample S with both contacts grounded. The cross section was milled with an FIB and the SKPM measurement was performed directly afterwards within the same apparatus. Note that the scale is different for x and y directions.

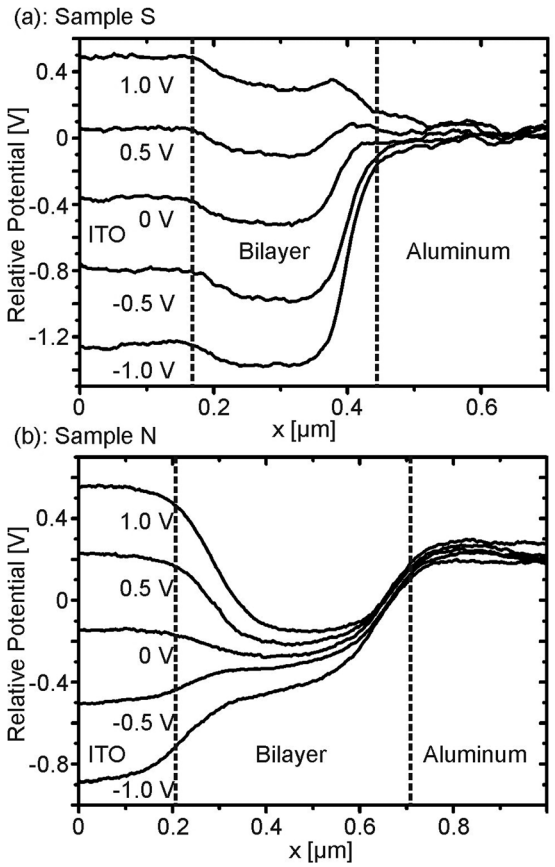

FIG. 3. Profiles of the surface potential through (a) sample S and (b) sample N for bias voltages between −1 V and 1 V. The positions of the ITO/P3HT and PCBM/Al interfaces are marked with vertical dashed lines.

the ITO contact and the P3HT and within the bilayer, pointing to a barrier at the ITO/P3HT interface and a non negligible series resistance within the P3HT/PCBM. In sample S, on the other hand, there is a voltage drop at the interface between PCBM and the aluminum exclusively. We can therefore conclude that the lower forward current and the S-shaped IV characteristics for sample S stem from a hindered charge transport between PCBM and the top contact. This result confirms the assumption of non ideal contacts being responsible for S-shaped IV-curves.[5,6] From Figures 3 and 4, one can see that the layer thickness in sample S amounts to about 200 nm and in sample N to about 400 nm. One could argue that the S-shaped characteristic results from this thin layer. However, we also fabricated bilayer solar cells with an organic layer thickness of 400 nm (batch 4, mentioned in the above paragraphs), which also showed S-shaped IV-curves and a potential barrier at the Al interface.

In summary, we compared P3HT/PCBM bilayer solar cells with normal and S-shaped IV-curves by *in-situ* SKPM measurements on their cross sections and could show that the S-shaped characteristic results from hindered charge

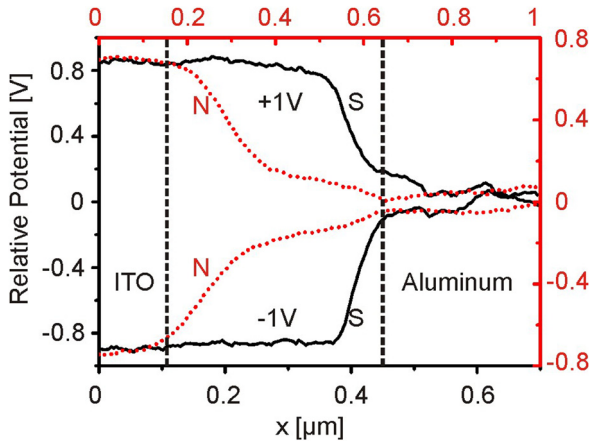

FIG. 4. Relative potential profiles for sample S (black solid line) and sample N (red dashed line) for an applied bias voltage of 1 V and −1 V, respectively. The lower x-axis and the left y-axis refer to sample S, the upper x-axis and the right y-axis refer to sample N. The positions of the ITO/P3HT and PCBM/Al interfaces are marked with vertical dashed lines.

transport at the PCBM/cathode interface. Our results lend additional credence to the importance of electrode interfaces as cause for S-shaped IV-curves and solar cell performance in general.

We acknowledge the German Federal Ministry of Education and Research (BMBF) for generous financial support (FKZ 13N10794 and FKZ 13N10723).

[1]I. Eisgruber, J. Granata, J. Sites, J. Hou, and J. Kessler, Sol. Energy Mater. Sol. Cells **53**, 367 (1998).
[2]C. Uhrich, R. Schueppel, A. Petrich, M. Pfeiffer, K. Leo, E. Brier, P. Kilickiran, and P. Baeuerle, Adv. Funct. Mater. **17**, 2991 (2007).
[3]A. Kumar, S. Sista, and Y. Yang, J. Appl. Phys. **105**, 094512 (2009).
[4]A. Wagenpfahl, D. Rauh, M. Binder, C. Deibel, and V. Dyakonov, Phys. Rev. B **82**, 115306 (2010).
[5]B. Y. Finck and B. J. Schwartz, Appl. Phys. Lett. **103**, 053306 (2013).
[6]B. Tremolet de Villers, C. J. Tassone, S. H. Tolbert, and B. J. Schwartz, J. Phys. Chem. C **113**, 18978 (2009).
[7]W. Tress, A. Petrich, M. Hummert, M. Hein, K. Leo, and M. Riede, Appl. Phys. Lett. **98**, 063301 (2011).
[8]A. L. Ayzner, C. J. Tassone, S. H. Tolbert, and B. J. Schwartz, J. Phys. Chem. C **113**, 20050 (2009).
[9]M. Pfannmoeller, H. Fluegge, G. Benner, I. Wacker, C. Sommer, M. Hanselmann, S. Schmale, H. Schmidt, F. A. Hamprecht, T. Rabe, R. Schroeder, and W. Kowalsky, Nano Lett. **11**, 3099 (2011).
[10]R. Saive, M. Scherer, C. Mueller, D. Daume, J. Schinke, M. Kroeger, and W. Kowalsky, "Imaging the electric potential within organic solar cells," Adv. Funct. Mater. (published online 2013).
[11]M. Scherer, R. Saive, D. Daume, M. Kroeger, and W. Kowalsky, AIP Adv. **3**, 092134 (2013).
[12]R. Saive, L. Mueller, E. Mankel, W. Kowalsky, and M. Kroeger, Org. Electron. **14**, 1570 (2013).
[13]M.-C. Wu, Y.-Y. Lin, S. Chen, H.-C. Liao, Y.-J. Wu, C.-W. Chen, Y.-F. Chen, and W.-F. Su, Chem. Phys. Lett. **468**, 64 (2009).
[14]D. S. H. Charrier, M. Kemerink, B. E. Smalbrugge, T. de Vries, and R. A. J. Janssen, ACS Nano **2**, 622 (2008).